Federico Galvanin*, Chun Fung Lee and Yuxuan Yang

11 On the development of pharmacokinetic models for the characterisation and diagnosis of von Willebrand disease

Abstract: Von Willebrand disease (VWD) is a metabolic disease characterised by a qualitative and/or quantitative deficiency of von Willebrand factor (VWF) a multimeric glycoprotein that mediates platelet adhesion in haemostatic processes. Pharmacokinetic (PK) models have been developed to characterise VWD metabolic pathways and to achieve a model-based diagnosis based on clinical data. However, current PK models cannot be calibrated from infusion tests data, and their calibration requires stressful 24-h long tests to be carried out on subjects to achieve a statistically satisfactory estimation of the individual haemostatic parameters. The objectives of this review chapter are the following: *i*) to provide a review on physiological modelling of VWD starting from the analysis of basic VWF mechanisms in the body; *ii*) to describe methods and modelling tools used to provide a model-based diagnosis of VWD and, consequently, a classification of complex VWD types; *iii*) to illustrate how model-based design of experiments (MBDoE) techniques can be applied to maximise the information that can be obtained from advanced clinical tests (DDAVP) but also from infusion tests used in VWD treatment where blood analogues are administered through single or multiple injections. Results show how PK models calibrated from clinical data can be used to estimate key haemostatic parameters in the diagnosis of the disease. Promising results on the application of MBDoE to design infusion tests show how the duration of clinical tests for the identification of key haemostatic parameters can significantly be reduced from 24 h to 2.5 h, with the potential to increase the acquired test information if multiple infusions can be managed.

Keywords: von Willebrand disease; pharmacokinetic models; model-based design of experiments

11.1 Introduction

Von Willebrand disease (VWD) is one of the most diffuse bleeding disorders in humans, caused by a modification of von Willebrand factor (VWF), a key multimeric glycoprotein present in the bloodstream and playing a crucial role in the haemostatic process [1]. VWF

***Corresponding author: Federico Galvanin**, Department of Chemical Engineering, University College London, London, UK, E-mail: f.galvanin@ucl.ac.uk

Chun Fung Lee and Yuxuan Yang, Department of Chemical Engineering, University College London, London, UK

As per De Gruyter's policy this article has previously been published in the journal Physical Sciences Reviews. Please cite as: F. Galvanin, C. F. Lee and Y. Yang "On the development of pharmacokinetic models for the characterisation and diagnosis of von Willebrand disease" *Physical Sciences Reviews* [Online] 2024. DOI: 10.1515/psr-2024-0058 | https://doi.org/10.1515/9783111394558-011

mediates platelet aggregation and thrombus growth, and binds, transports and protects coagulation factor VIII. VWD-induced alteration of VWF in the bloodstream causes symptoms ranging from sporadic or prolonged bleeding episodes, nosebleeds, bleeding from small lesions in skin, mucosa or the gastrointestinal tract, menorrhagia and excessive bleeding after traumas, surgical interventions or childbirth [2, 3]. According to the 2019 survey from the World Federation of Hemophilia, there are approximately 80000 confirmed cases of VWD worldwide [4]. This value is far lower than the expectation of 1 % global prevalence, which historically leads to only 0.1 % of disease carriers being diagnosed [5]. The low diagnosis rate is generally attributed to the complexity of the standard diagnosis procedures. The diagnosis requires numerous laboratory tests requiring the clinician's interpretation [6]. Human error and bias could lead to misdiagnoses with consequence that might be fatal, and this motivates the development of systematic approaches for VWD diagnosis. Diagnosis of VWD is a complex task due to the heterogeneous nature of the disorder, characterised by a number of VWD types and subtypes [7]. Subjects affected by VWD are usually classified into three VWD possible types on the basis of having a partial (type 1), total (type 3) quantitative defect or a qualitative deficiency in plasma VWF (type 2) [1]. Whilst VWD type 2 and type 3 are straightforward to diagnose, as they involve a variety of qualitative defects on VWF (VWD type 2) or the total absence of VWF (VWD type 3), the diagnosis of VWD type 1, which represents the most common VWD type (accounting for the 75 % of all cases), may become a long and very complicated task because of the elusive nature of the disease. Diagnosing type 1 VWD poses several challenges because of the strong heterogeneous nature of the disorder and the high intra-subject variability observed in the haemostatic laboratory findings. Recent studies involving 24 h 1-desamino-8-d-arginine vasopressin (DDAVP) tests carried out on a genetically categorised population of subjects underlined the importance of impaired VWF secretion and elimination from the body in modulating type 1 VWD and the key role of genetic mutations that are still not easily understood [8]. Type 2 VWD is characterised by different subtypes: 1) Type 2A, where the binding of VWF with platelets is reduced because of discriminatory deficiency of high molecular weight multimers, which has better ability in blood clotting, the potential cause being that specific mutations increase the susceptibility of large multimers to reduce to low multimers in plasma; 2) Type 2B, where VWF prematurely binds with the platelets, which enhance the removal of both platelet and VWF from plasma before reaching the wound; 3) Type 2M, where the binding between platelet and VWF is decreased, which reduces probability of platelets to clot in the injured site; 4) Type 2N, where as a result of a genetic mutation, the VWF binding with the protein Factor VIII is impaired, and this reduces the probability of blood clotting in the injured site.

Acquired von Willebrand syndrome (AVWS) is a rare heterogeneous bleeding disorder [9] similar to inherited VWD that occurs in patients with no personal or family history of bleeding. AVWS is not a result of genetic defects but may be caused by underlying pathological conditions, including lympho- and myeloproliferative disorders, solid tumours, immune diseases, cardiovascular disorders, hypothyroidism, diabetes,

and infectious diseases, or the side effects of drugs [10]. Subjects affected by AVWS present severe bleeding symptoms requiring urgent and often multiple treatment [9].

Pharmacokinetic (PK) models of different degree of complexity have been recently proposed for the characterisation of VWD, starting from algebraic models [11] to models described by differential and algebraic equations (DAEs) characterising the multimeric VWF patterns in VWD [12–15] and AVWS [10]. The calibration of these models is based on the estimation of subject-specific haemostatic parameters to elucidate the critical pathways involved in the disease characterisation and to assist model-based approaches to VWD diagnosis [13, 16]. However, the complexity of these models, defined by the number of state variables and subject-specific parameters, might require the execution of advanced, time-consuming (24 h long) and cumbersome non-routine tests like the DDAVP (desmopressin) response test to achieve a precise estimation of the individual haemostatic parameters. DDAVP test is a dynamic test where desmopressin is administered subcutaneously at a prescribed dose to patients (0.3–0.4 μg/kg body weight) [10, 17], and blood samples are collected at regular fixed times to characterise the subject's response. DDAVP is also used in the treatment of severe forms of VWD as desmopressin is capable of inducing a fast release of VWF stored in the Weibel Palade bodies of the endothelial cells. The time course of VWF antigen (VWF:Ag) and VWF collagen binding (VWF:CB) can be quantitatively analysed using dynamic kinetic models to characterise the time variation of VWF concentration in plasma [17]. VWF kinetics depend on three key factors: *i*) the amount of VWF released and the rate of release; *ii*) VWF proteolysis, i.e. the reduction of VWF multimeric chains into smaller multimeric forms as a result of the activity of a specific enzyme (ADAMTS-13); and *iii*) VWF elimination from the blood stream (clearance). As illustrated in Budde et al. [18], DDAVP administration is not suitable to treat all the types of VWD and is not recommended in patients with specific co-morbidities including atherosclerosis, heart failure or other conditions requiring diuretic treatment, as well as in very young children or in patients older than 65–70 years. For these reasons, plasma-derived VWF/FVIII analogues [19] are nowadays the current standard for controlling acute bleeding episodes or as prophylaxis for invasive or surgical procedures. Available VWF concentrates differ in their purification and pathogen removal as well as in VWF multimeric concentration and activity [20], all aspects which affect therapeutic safety and efficacy. So far there have been limited specific studies on models specifically developed to characterise the kinetics of exogenous VWF infusion of VWF concentrates [21] and to quantify the intrinsic information that can be obtained from infusion tests when different VWF concentrates are used. A key challenge in the identification of physiological models of VWD is the precise estimation of the set of subject-specific haemostatic parameters from potentially limited amount of data, and the evaluation of their 'estimability'. Estimability is strictly related to the level of information acquired from clinical tests and to the protocol used for dynamic model calibration [22].

This chapter is structured as follows: in Section 11.2, routine and advanced tests used in the clinical diagnosis of VWD are introduced; Section 11.3 presents the fundamental mechanisms involved in the disease characterisation; Section 11.4 provides an overview of

procedures for model-based diagnosis, including PK model formulation (Section 11.4.1), the problem of estimating metabolic parameters from data (Section 11.4.2), and the development of new kinetic model including VWF exogenous infusion (Section 11.4.3). Section 11.5 illustrates results on the application of model-based diagnosis to subjects affected by VWD, while Section 11.6 illustrates fundamentals in the application of model-based design of experiments techniques (MBDoE) [23, 24] for the design of VWF infusion tests used in the treatment of VWD. Results reported in Section 11.7 on AVWS subjects show the potential of optimally designed infusion tests in drastically decreasing the time and effort required for a precise identification of the key set of haemostatic parameters. Section 11.8 draws some final conclusions on the research in the area and future challenges.

11.2 Clinical diagnosis of von Willebrand disease

A guidance publishes from the National Heart, Lung and Blood Institute [6] gives a standard procedure for diagnosing VWD. Since VWD is an inherited disease, the procedure begins with reviewing the medical history of the patient's family and relatives. Preliminary haemostasis tests are then carried out including platelet count, partial thromboplastin time and prothrombin time. If the haemostasis test result is negative, the patient should be referred to other specialists; otherwise, initial VWD assays will be performed to classify the type of VWD. VWD assays include four main items:

1. VWF antigen (VWF: Ag) assay: shows the total VWF concentration in plasma regardless of the multimer molecular weight.
2. VWF Ristocetin Cofactor Activity (VWF: RCo) assay: to measure the degree of platelet agglutination induced after the addition of ristocetin.
3. Factor VIII: a blood-clotting protein that is essential in the coagulation process.
4. VWF collagen-binding assay (VWF: CB): to measure the binding of VWF to type I and III collagens. High molecular weight multimers have a higher affinity to collagen, so VWF:CB represents a measure of the concentration of high molecular weight VWF multimers in plasma. All these tests are routine tests usually carried out at basal, stationary conditions. In diagnosing VWD, VWF: RCo assay can be partially replaced by the VWF: CB assay [25] because the VWF: RCo assay is time-consuming, and the result particularly difficult to reproduce [5]. Since the collagens favourably attaches to the larger multimer, the VWF: CB result is useful to discriminate the types of VWD that are insufficient in large multimers such as type 1, 2A and 2B. If all these tests failed to give a clear diagnosis, one or more *advanced laboratory tests* are required. These tests are very assorted, but there are some common options followed in the clinical practice [6]:
    1. Measurement of multimer distribution patterns by gel electrophoresis;
    2. The VWF Ristocetin Cofactor Activity (VWF: RCo);
    3. The binding of factor VIII to VWF;
    4. Desmopressin (DDVAP) test;
    5. DNA sequencing.

The identification of the VWD type might become a long and cumbersome procedure, as it largely depends on the experience of the clinician and the subjective ability to systematically analyse the results from routine and advanced tests. When analysing the results, the clinician might potentially ask to repeat some of the tests if needed to then provide a clear identification of the disease through differential diagnosis.

11.3 From fundamental mechanisms to VWD modelling

Figure 11.1 describes the base mechanisms involved in the distribution of VWF in the bloodstream from the production to elimination [13]. After VWF is synthesised in the ethnophiles cell as ultra-large multimers, there are three basic mechanisms taking place:

1. VWF release: the ultra-large VWF multimers are released into the plasma.
2. VWF proteolysis: the enzyme ADAMTS13 splits the ultra-large multimers into shorter chains, which are the low molecular weight VWF multimers.
3. VWF elimination (even known as *VWF clearance*): all multimers are removed from plasma in the liver eventually with a mechanism that does not depend on multimer size.

Any irregularity in these steps can lead to low VWF levels or abnormal multimer distribution hence different types of VWD.

Figure 11.2a and 11.b shows an example of data collected from DDAVP clinical tests for O healthy subjects and a subject affected by AVWS in terms of VWF antigen (VWF:Ag) and VWF collagen binding (VWF:CB). Clinical data have from DDAVP been supplied by the Hospital of Padua. DDAVP (1-desamino-8-D-argine vasopressin; Emosint, Sclavo, Italy) was

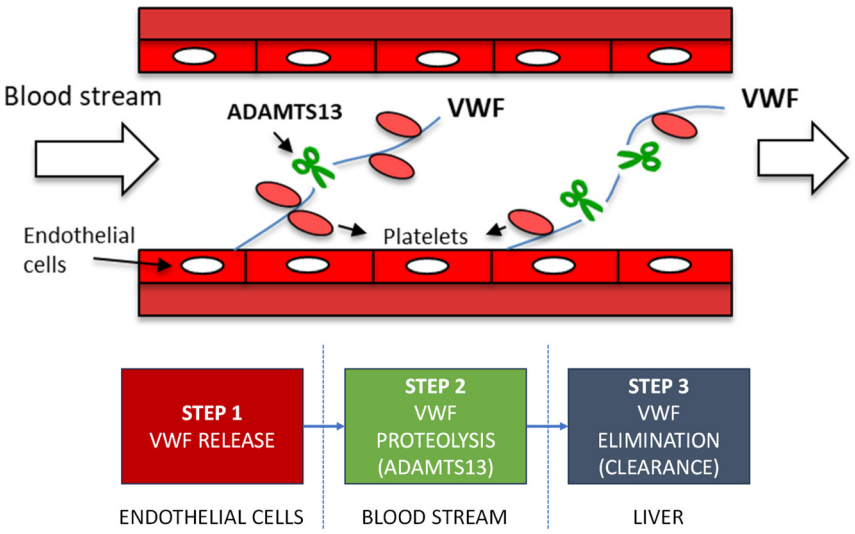

Figure 11.1: Base mechanisms involved in the distribution of VWF in the bloodstream.

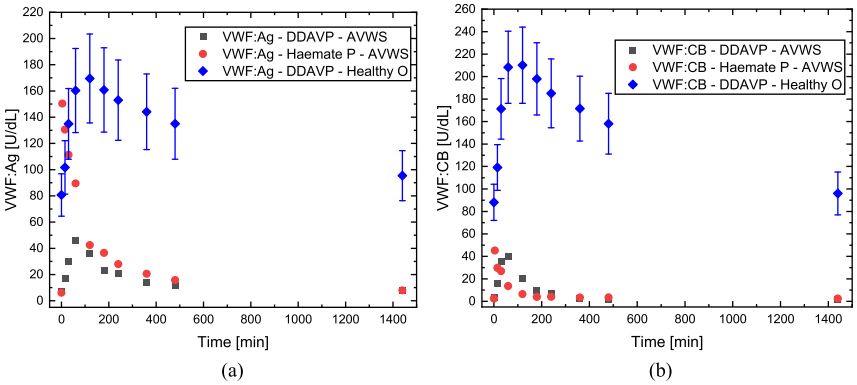

Figure 11.2: Examples of (a) VWF:Ag and (b) VWF:CB measurements after DDAVP administration to healthy O (blue diamonds), AVWS subject (black squares) and after VWF analogue (Haemate P) administration for a subject affected by AVWS (red circles) [21].

administered subcutaneously at a dose of 0.3 μg kg^{-1}. Blood samples were collected before and 15, 30, 60, 120, 180, 240, 480 min and 24 h after administering DDAVP for a pool of health subjects (O/non-O blood group) and for a subject affected by AVWS. AVWS patient and normal subjects were studied in accordance with the Helsinki Declaration, after obtaining their written informed consent, and our ethical board's approval of the study. The same subject was also treated with exogenous intravenous administration of Haemate P, a VWF concentrate commonly used in the treatment of VWD. After administering 2,000 U of Haemate P (a VWF analogue) (Behring GMBH, Hattersheim am Main, Germany), blood samples were collected at 4, 15, 30, 60, 120, 180, 240, 360, 480 min and at 24 h. In clinical practice, sampling points are concentrated at the beginning of the test, as intravenous administration produces faster dynamics in VWF as compared to subcutaneous DDAVP administration. As VWF exists across a multimeric range, VWF:Ag represents a measure of the overall VWF amount in plasma for the subjects, including high and low molecular weight VWF species, while VWF:CB is a measure of the amount of high molecular weight species only.

There are several important aspects to observe from Figure 11.2:

- All curves show a peak that corresponds to the maximum in VWF release in overall terms (VWF:Ag, Figure 11.2a) and in terms of high molecular weight multimers (VWF:CB, Figure 11.2b)
- After the peak, a slower decay is observed in VWF:Ag as compared to VWF:CB caused by the proteolytic activity (i.e. a fraction of high molecular weight multimers is reduced to multimers with shorter chains). This is valid for both healthy O subjects and subjects affected by AVWS.
- AVWS is characterised by significantly reduced VWF:Ag and VWF:CB levels before and after DDAVP administration (levels are considerably low also at basal state, i.e. see values at t = 0 min when compared to healthy O subjects);

- The infusion of Haemate P in the AVWS patient prompted a sudden increase in low molecular weight species (see VWF:ag peak in the first observation after 4 min) but produced a limited release of high multimeric species (relatively low VWF:CB levels) during the test;
- For the AVWS patient, very low VWF:CB levels are observed both after DDAVP and after Haemate P infusion;
- The infusion of Haemate P forces a very fast dynamic VWF response, i.e. by 240 min after the administration most of the VWF:CB was no longer detectable.

Since high molecular weight multimers are more active in the coagulation process, and their deficiency leads to prolonged bleeding in subjects even after small lesions or scars. It is of primary importance to understand: *i*) if and how infusion tests can be used for the identification of subject-specific metabolic parameters; *ii*) if infusion tests can be more or less informative than a standard DDAVP test, i.e. if this test can provide a more precise and accurate estimation of haemostatic parameters; *iii)* if the infusion protocol can be personalised and optimally designed; *iv)* given that a conventional DDAVP requires 24 h to be execute, if the overall test duration can be shortened by adopting infusion tests, preserving at the same time the required level of information.

11.4 Model-based diagnosis of VWD

A model-based procedure for VWD diagnosis based on the quantitative characterisation of the metabolic pathways involved in post-DDAVP and VWF infusion studies is illustrated in Figure 11.3. Given the availability of historical data for each subject class, the variance of the population can be characterised by estimating the parameters of a

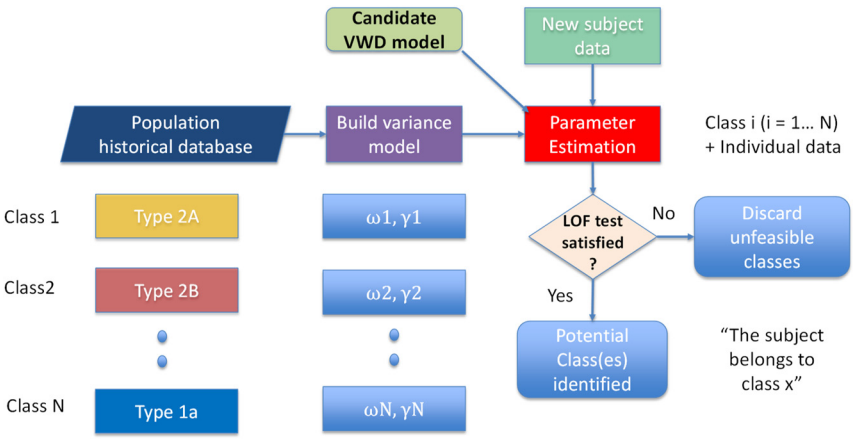

Figure 11.3: Procedure used for model-based diagnosis.

heteroscedastic model (see Section 11.4.2, equation (11.15)). When test data are available for the unknown subject, a parameter estimation is carried out to estimate the set of kinetic parameters of a candidate model, based on both historical data from each subject's class and individual data [13]. The class providing the lowest lack-of-fit (LOF) statistics represents the class of belonging, as it evaluates both the deviation between model predictions and individual test data (residuals, see Section 11.4.2, equation (11.15)) and the distance from the population data.

The following sections contain a description of the pharmacokinetic models used for model-based diagnosis (Section 11.3.1) and the identification of metabolic parameters from DDAVP data (Section 11.3.2) and exogenous infusion data (Section 11.3.3).

11.4.1 Pharmacokinetic models of VWD

One-compartmental models with first order input and output kinetics are used to investigate the time course of VWF:Ag (or VWF:CB) concentration after DDAVP administration [26]. These models take the algebraic form

$$y^{AG} = A\left(e^{-k_e(t-\tau)} - e^{-k_0(t-\tau)}\right) + B \tag{11.1}$$

where y^{AG} is the VWF:Ag concentration ([U/dL]), A represents the intercept ([U/dL]) and B ([U/dL]) the VWF baseline calculation, while k_0 and k_e are the release and elimination parameters, respectively. A lag time phase in both release and elimination does exist and is represented by the constant τ. The relevant pharmacokinetic (PK) parameters that can be obtained from (1) are the amount of VWF:Ag released after DDAVP administration (Q), the elimination half-life ($T_{1/2}$, [h]), plasma clearance (CL, [mL/kg/h]) and velocity of release (V_{re} [U/kg/h]). Their expressions are

$$Q = AV_d\frac{(k_0 - k_e)}{k_0} \tag{11.2}$$

$$T_{1/2} = \ln 2/k_e \tag{11.3}$$

$$CL = k_e V_d \tag{11.4}$$

$$V_{re} = Bk_e V_d \tag{11.5}$$

where V_d is the distribution volume evaluated following Menache and coworkers [27] (V_d = 40 mL/kg). Average values for (2–5) PK parameters are usually expressed as means ± standard error of the mean. The model has been applied in clinical practice to quantitatively analyse both VWF:Ag and VWF:CB data from clinical trials and provided useful insights on pharmacokinetics of different VWD types [26]. However, a strong limitation of the model (1) is that it aims at characterising either the overall amount of VWF (defined by VWF:Ag) or the amount of high molecular weight multimers (VWF:CB) by simply modelling the balance between the release of VWF from endothelial cells and

its removal from the blood circulation. The model does not provide any information about the relative abundancy of high or low molecular weight multimers in the blood stream defining the multimeric distribution of VWF in plasma and conditioning the haemostatic activity of the subject affected by the disease. The extent of modification of VWF multimer distribution reflects the competition between clearance and proteolysis by means of ADAMTS13.

A mechanistic PK model for the description of VWD was first proposed by Galvanin et al. [13] to describe the proteolysis mechanism and to quantify the distribution and relative concentration of different multimeric species in subjects affected by VWD. A model scheme is reported in Figure 11.4a. After DDAVP administration, a three-step mechanism is known to occur [27]:

1. Release of super ultra large multimers (SUL); the release rate and amount are subject-dependent;
2. Proteolysis of SUL to smaller species by means of ADAMTS13: SUL multimers can be cleaved to high (HMW), ultra-large (UL) or low (LMW) molecular weight multimers;
3. Clearance (i.e. multimer elimination from plasma), taking place at the liver level and independent of the multimer size.

For each subject, the release rate is determined by the value of k_0 [min^{-1}]; the rate of proteolysis of SUL, UL and HMW to lower molecular weight species is described by parameters k_i, while the elimination rate for both UL, HMW and LMW is defined by k_e [min^{-1}].

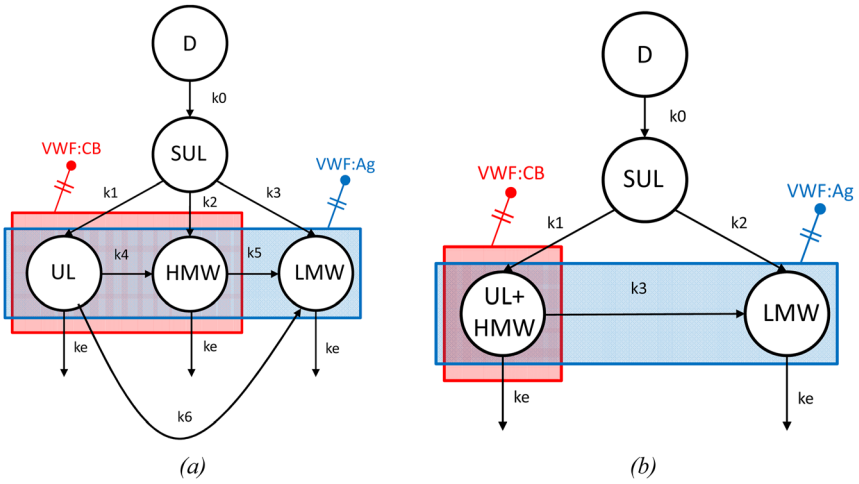

Figure 11.4: Structure of the mechanistic models used for model-based VWD diagnosis: a) original model by Galvanin et al. [13]; b) simplified model. VWF:Ag and VWF:CB measurements are indicated by the blue and red box, respectively.

The model was remarkably efficient to represent the variability observed in healthy subjects, 2A, 2B and Vicenza subjects and allowed to perform a model-based diagnosis based on estimated model parameters [13]. However, it required multimeric assays using gel electrophoresis to quantify the amount of UL in plasma after DDAVP. This measurement is essential for a precise estimation of the proteolytic parameters for a single subject, as parameters k_1 and k_4 are not identifiable from VWF:Ag and VWF:CB data only. Data from multimeric analysis are usually difficult and expensive to obtain, as they require a specific knowledge on the electrophoresis techniques and a significant effort in terms of analytical resources. For this reason, the model complexity was reduced to develop the model represented in Figure 11.4b. The simplified model was developed under the following physiological assumptions:

a) At the basal state, both HMW and LMW multimers are present, but SUL concentration is zero;
b) SUL multimers cannot be measured directly from VWF measurements, and their release is only a consequence of DDAVP administration;
c) Only a compartment quantifying the sum of UL and HMW can be fully characterised, and these multimers can be cleaved to LMW multimers.

It is assumed that only the sum of HMW and LMW multimers can be evaluated from VWF:Ag measurements, while VWF:CB measurements are exclusively imputed to the (UL + HMW) amount. The proposed mechanistic model allows for the evaluation of standard pharmacokinetic parameters including Q, $T_{1/2}$, CL, V_{re} and the evaluation of the velocity of VWF removal V_{el} [U/kg/h] as in equations (11.1)–(11.5). More importantly, it allows the quantitative evaluation of VWF levels involved in the proteolytic channels thanks to the estimation of k_1, k_2 and k_3 parameters. The model was extremely efficient on identifying subjects affected by VWD for well-characterised subjects (see Table 11.1) aligning with the results from differential diagnosis, but failed to clearly distinguish between borderline healthy cases (see shaded area in the table), particularly when parameters k_1 and k_2 were estimated with large uncertainty.

Table 11.1: Example of model-based diagnosis results using the simplified model reported in Galvanin et al. [13]. Columns represent the values of chi-square obtained from the LOF related to each class. Minimum chi-square value for each identified class is indicated in bold. Shaded cells indicate uncertainty in classification.

Test subject	Differential diagnosis	LOF test (χ^2 test)				Model-based diagnosis
		O	*Non-O*	*2B*	*Vicenza*	
C	Vicenza	107	102	133	**35**	**Vicenza**
D	Non-O	1236	**1229**	1958	5083	**Non-O**
E	Non-O	5350	**3409**	7268	9148	**Non-O**
F	2B	92	87	**20**	177	**2B**

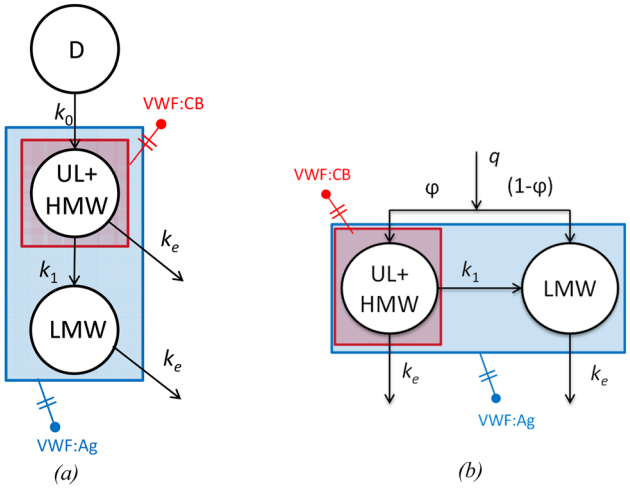

Figure 11.5: Simplified compartmental models of VWD. (a) Structure of the post-DDAVP model of VWD proposed by Ferrari et al. [14] representing the distribution of ultralarge + high (UL + HMW) and low molecular weight (LMW) multimers in the blood; (b) structure of the model proposed by Galvanin et al. [21] including exogenous VWF infusion, where q is the infusion rate [U/min] and φ is an effective partition constant defining the split between (UL + HMW) and LMW. Accessible compartments through VWF:Ag and VWF:CB measurements are indicated by the blue and red box, respectively.

The Ferrari and coworkers [14] dynamic model represents a further simplification of the original model and has been developed to represent the evolution in time of different multimeric species after DDAVP administration from VWF:Ag and VWF:CB data. The model assumes that *i*) the proteolysis of SUL is extremely fast, so that the SUL compartment can be neglected; *ii*) SUL can only decompose to (UL + HMW). The model is a simplification of the model by Galvanin et al. [13] but, unlike the original model, is structurally identifiable from VWF:Ag and VWF:CB data, i.e. model parameters can always be precisely estimated from DDAVP clinical data. This makes the model more suitable to investigate heterogeneous VWD forms, such as type 1 VWD, where the probability of incurring into false negatives during a differential diagnosis is higher. This model structure is illustrated in Figure 11.5a and the mathematical details are reported in Section 11.4.2.

The model of Ferrari and coworkers [14] can only represent release after subcutaneous DDAVP administration, and assumes that all the VWF is released from endothelial cells after a standard DDAVP dose is administered. To overcome this limitation, a new pharmacokinetic model has been proposed by Galvanin et al. [21] to explicitly include exogenous VWF administration as reported in Figure 11.5b. In this model, the partition constant φ is introduced to consider the possibility to administer different VWF analogues, characterised by a different relative concentration of (UL + HMW) and LMW multimers. This model is detailed in Section 11.4.3.

11.4.2 Identification of haemostatic parameters from DDAVP tests

The model assumes that after DDAVP administration, both high molecular weight (HMW) and ultralarge molecular weight (UL) VWF multimers are released from the endothelial cells. Then, HMW and UL multimers are cleaved to low molecular weight (LMW) multimers by the metalloprotease ADAMTS-13 before being finally eliminated from the bloodstream. This model is described by a system of differential and algebraic equations (DAEs)described by equations (11.6)–(11.11). Differential equations are written as

$$\frac{\mathrm{d}x^{\mathrm{UL+HMW}}}{\mathrm{dt}} = k_0 D\,\mathrm{e}^{-k_0(t-t_{\max})} - k_1\left(x^{\mathrm{UL+HMW}} - x_b^{\mathrm{UL+HMW}}\right) - k_{\mathrm{e}}\left(x^{\mathrm{UL+HMW}} - x_b^{\mathrm{UL+HMW}}\right) \tag{11.6}$$

$$\frac{\mathrm{d}x^{\mathrm{LMW}}}{\mathrm{d}t} = k_1\left(x^{\mathrm{UL+HMW}} - x_b^{\mathrm{UL+HMW}}\right) - k_{\mathrm{e}}\left(x^{\mathrm{LMW}} - x_b^{\mathrm{LMW}}\right) \tag{11.7}$$

where $x^{\mathrm{UL\ +\ HMW}}$ and x^{LMW} are the amount of UL + HMW and LMW multimer units [U] contained in the plasma; the subscript b refers to the basal state (i.e. the state of the subject before the DDAVP test starts); t is the test execution time and $t_{\max}$ is the time at which the release profile peaks. In the kinetic model, k_0 [min^{-1}] represents the kinetics of VWF release from endothelial cells; k_1 [min^{-1}] the proteolytic conversion of large and ultra-large VWF multimers into LMW multimers and k_{e} [min^{-1}] represents the clearance of VWF from the circulation, which is assumed to be the same for both the UL + HMW multimers and the LMW multimers [28]. The amount of VWF released, Q^{DDAVP} [U], can be calculated from

$$Q^{\mathrm{DDAVP}} = \int_0^{\tau} k_0 D e^{-k_0(t-t_{\max})} dt \tag{11.8}$$

where D [U/dL] is a release parameter and τ is the overall test duration [min]. It is important to notice that, for a given subject, parameter k_0 quantifies the rate of release, while D is related to the amount of VWF released from the endothelial cells after a standardised DDAVP dose of 0.3 µg/kg body weight. A limitation of this model is that it does not include the amount of DDAVP administered to the subject as explicit variable. The measured responses are the antigen concentration y^{AG} [U/dL] and collagen binding concentration y^{CB} [U/dL], which are defined, respectively, by the following algebraic equations:

$$y^{AG} = \frac{\mathrm{x}^{\mathrm{UL+HMW}} + \mathrm{x}^{\mathrm{LMW}}}{V_d} \tag{11.9}$$

$$y^{CB} = \frac{\mathrm{x}^{\mathrm{UL+HMW}}}{V_d} \tag{11.10}$$

It is assumed that VWF:CB measurements can quantify the amount of UL and HMW multimers in plasma, while VWF:Ag measurements quantify the overall amount of VWF multimers (i.e. UL + HMW + LMW). A correction was introduced in the definition of the

collagen binding measurements in order to account for the different affinity of multimers to collagen observed in clinical tests using the following algebraic equation:

$$y^{CB'} = k y^{CB} \frac{y_b^{AG}}{y_b^{CB}} \tag{11.11}$$

where k is a correction factor to be estimated from data, and y_b^{AG} and y_b^{CB} are antigen and collagen binding concentration measurements [U/dL] determined at basal state. In (11.9) and (11.10), V_d = 40 mL/kg_{bw} is the approximate distribution volume again evaluated according to Menache et al. [27]. Initial conditions for differential state variables (i.e. at t = 0) can be calculated from basal antigen and collagen binding concentrations:

$$x(0) = \left[x_b^{\mathrm{UL+HMW}} x_b^{\mathrm{LMW}} \right] = \left[y_b^{CB} V_d y_b^{AG} V_d - y_b^{CB} V_d \right] \tag{11.12}$$

The full set of model parameters to be estimated from available post-DDAVP VWF:Ag and VWF:CB measurements is $\boldsymbol{\theta}^{\mathbf{DDAVP}} = [k_0 \quad k_1 \quad k_e \quad D \quad k \quad y_b^{CB} \quad t_{\max}]$. The DDAVP test needs to be carried out on each single subject [14] to achieve a statistically precise estimation of the individual kinetic parameters to accurately quantify the rate of VWF release, proteolysis and elimination from plasma. Nonlinear parameter estimation results are assessed in terms of estimated values and a-posteriori statistics including t-values and confidence intervals. For a statistically precise estimation, the t-value for each model parameter is calculated from

$$t_i = \frac{\hat{\theta}_i}{\sigma_{\theta_i}} i = 1 \ldots N_\theta \tag{11.13}$$

where $\hat{\theta}_i$ represents the estimated value from maximum likelihood parameter estimation and σ_{θ_i} the corresponding standard deviation. Each t-value calculated from (11.13) is compared against a tabulated reference t-value related to $(N - N_\theta)$ degrees of freedom and 95 % confidence level, where N is the total number of test samples and N_θ the total number of model parameters. A t-value higher than the reference t-value indicates a precise parameter estimation. Model adequacy is evaluated using a lack-of-fit (LOF) χ^2 test, by comparing the calculated chi-square

$$\chi^2 = \sum_{i=1}^{N} \frac{r_i^2}{\sigma_i^2} \tag{11.14}$$

with a tabulated reference chi-square at a 95 % confidence level for $(N - N_\theta)$ degrees of freedom (χ^2_{ref}) [29]. In (11.14), r_i and σ_i^2 are, respectively, the residual (difference between measured value and model prediction) for the i-th observation and the corresponding variance of measurement error. If $\chi^2 < \chi^2_{\mathrm{ref}}$, the model is adequate to represent the test data. The heteroscedastic relative variance model equation

$$\sigma^2 = \omega^2 (y^2)^\gamma \tag{11.15}$$

is used to estimate the variability in the test response y (VWF:Ag or VWF:CB) at each time point. The variance is quantified at the level of the single individual and of the population of subjects (for the population y represents the average response for each class of subjects), by estimating parameters ω and γ directly from data.

11.4.3 Models including exogenous infusion of VWF concentrates

In the infusion models, VWF is distributed among the (UL + HMW) and LMW compartments, and the release from endothelial cell is assumed to be negligible, as illustrated in Figure 11.5b. The model is represented by the following differential equations

$$\frac{\mathrm{d}x^{\mathrm{UL+HMW}}}{\mathrm{dt}} = \varphi q - k_1\left(x^{\mathrm{UL+HMW}} - x_b^{\mathrm{UL+HMW}}\right) - k_{\mathrm{e}}\left(x^{\mathrm{UL+HMW}} - x_b^{\mathrm{UL+HMW}}\right) \tag{11.16}$$

$$\frac{\mathrm{d}x^{\mathrm{LMW}}}{\mathrm{d}t} = (1-\varphi)q + k_1\left(x^{\mathrm{UL+HMW}} - x_b^{\mathrm{UL+HMW}}\right) - k_{\mathrm{e}}\left(x^{\mathrm{LMW}} - x_b^{\mathrm{LMW}}\right) \tag{11.17}$$

where φ is the effective partition constant, representing the relative amount of high and low molecular weight multimers that are present in the injected dose, which is specific for each VWF concentrate and can be calculated from the specific collagen binding capacity

$$\varphi = \frac{VWF:CB^{IV}}{VWF:Ag^{IV}} \tag{11.18}$$

where $VWF{:}CB^{IV}$ and $VWF{:}Ag^{IV}$ are collagen binding and antigen VWF measurements carried out on the infused VWF concentrate. Intravenous administration is modelled through the infusion rate q [U/min]:

$$q = \begin{cases} D^{IV} & t \le t_{inj} \\ 0 & t_{inj} < t \le \tau \end{cases} \tag{11.19}$$

In (11.19), D^{IV} is the discrete injection rate [U/min] and t_{inj} is the injection time [min]. The model is subject to the following additional constraint on infusion dose:

$$Q^{IV} = \int_0^{\tau} q dt \tag{11.20}$$

where Q^{IV} is the actual injected dose of VWF concentrate [U]. The full model is constituted by the system of differential and algebraic equations (11.16)–(11.20) including (9-10) and (11) to be solved with the initial conditions provided by (11.12). For this model, the full set of model parameters to be estimated from VWF:CB and VWF:Ag data is

$$\theta^{\mathrm{IV}} = \left[\, k_1 k_e D^{IV} k y_b^{CB} t_{inj} \right] \tag{11.21}$$

The parameter sets in both models (i.e. $\boldsymbol{\theta}^{\mathbf{DDAVP}}$ and $\boldsymbol{\theta}^{\mathbf{IV}}$) are determined for each subject by iteratively solving a nonlinear optimisation problem based on maximum likelihood

parameter estimation [30] following the procedure described in Taverna et al. [15] and carried out using the commercial software gPROMS® ModelBuilder [31]. VWF:Ag and VWF:CB measurements are assumed to be normally distributed with a standard deviation of 2 U/dL as evaluated from repeated measurements on the AVWS subject, as reported in Galletta et al. [10].

11.5 Model-based diagnosis of VWD subjects

Given the availability of VWD:Ag and VWF:CB historical data, it is possible to characterise the variability in the population by estimating the parameters of the heteroscedastic variance model (15) as reported in Table 11.2. Results show a significantly higher variability in healthy subjects characterised by O blood group, as indicated by the higher value of ω. Results reported in Table 11.3 show the estimated values of PK parameters using the Ferrari et al. [14] model for healthy subjects with O and non-O blood group, 2A,

Table 11.2: Estimated parameter values of the heteroscedastic variance model used to describe the population of subjects as in equation (11.15).

Response	Parameter	Healthy O	Healthy non-O	Vicenza	2B
VWF: Ag	ω	0.63	5.51	0.59	0.48
	γ	0.5	0.18	0.66	0.67
VWF: CB	ω	0.28	2.55	0.24	0.2
	γ	0.69	0.34	0.89	1.08

Table 11.3: Estimation of PK parameters for the Ferrari et al. [14] model from population data obtained for healthy subjects (O, non-O), 2A, 2B and Vicenza subjects. Values in bold indicate critical values for selected VWD types.

Model parameter	Subject's class				
	Healthy O	Healthy non-O	2B	Vicenza	2A
D	17.586	117.912	716.066	682.427	821.996
k	1.0382	0.9317	0.2399	0.6453	0.2451
k_0	0.0233	0.0260	0.0045	0.0093	0.0023
k_1	0.0003	0.0001	**0.0077**	**0.0121**	**0.0061**
k_e	0.0016	0.0007	0.0094	**0.0335**	0.0115
$t_{\max}$	124.244	47.837	77.990	57.818	264.468
y_b^{CB}	57.5759	85.1613	25.8928	4.7951	21.9648
$\chi 2$ (χ_{ref}^2)	13.2603	3.6782	6.5063	2.51614	0.610841
	(24.9958)	(24.9958)	(24.9958)	(24.9958)	(24.9958)

2B and Vicenza subjects. Results reflect the physiological profile of the different VWD types: i) Vicenza subjects (a specific type 1 form) show highly increased elimination and proteolytic activity (k_e and k_1 parameters, respectively), as well as reduced release (low k_0 value) compared to healthy subjects; ii) 2A and 2B subjects show increased proteolysis, with subjects 2A being characterised by an extremely low release rate (low k_0) and high elimination (high k_e). This underlines the severity of 2A forms, as the subjects are characterised by very low VWF levels in the blood stream

As illustrated in Figure 11.6a, the quantification of key haemostatic parameters *CL* (clearance, equation (11.4)) and *Q* (amount of VWF released, equation (11.8)) shows a clear distinction between healthy subjects and 2A, 2B and Vicenza subjects, while for type 1 VWD subjects, classification results show a more fragmented behaviour. It is also important to observe the proximity of some type 1 subjects to healthy subjects, which makes the classification particularly challenging. The analysis can be extended by including genetic information on specific mutations of VWF genes characterising each subject (Figure 11.6b), which allows to identify mutations (C1130, 1534–3) that are responsible of increased elimination from the blood stream (high clearance).

The availability of a subject-specific calibrated model allows for the quantification of the amount of (UL + HMW) and LMW released after a DDAVP test. This can be quantified by the area under the x^{L} and x^{UL+H} curves. Interestingly, this analysis underlines the existence of clear data clusters, as reported in Figure 11.7, in the definition of type 1 VWD subtypes. Three specific clusters could be identified:

1. Type 1A (purple balls): characterised by low levels of VWF released and low concentrations of both HMW and LMW multimers in plasma, higher than normal VWF clearance (associated with mutations R1205H, C1130G/F/R, W1144G);

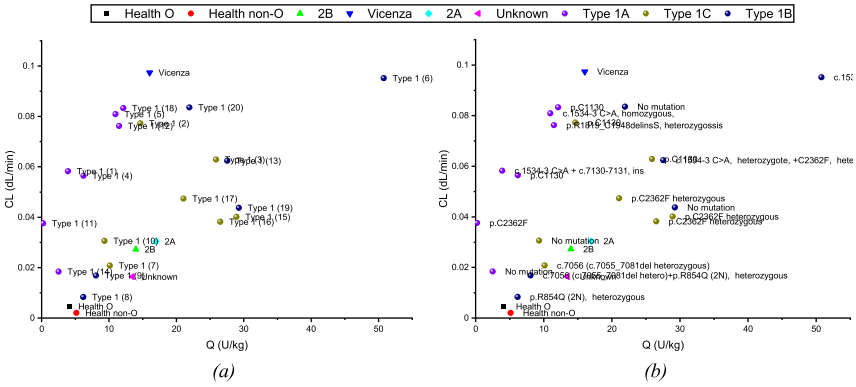

Figure 11.6: Clearance (CL) Vs amount of VWF released (Q) for (a) healthy subjects, 2A, 2B, Vicenza and selected type 1 individual subjects and (b) graphs including specific subjects mutations. Type 1 subjects are labelled in three distinct subtypes: type 1A, 1B and 1C.

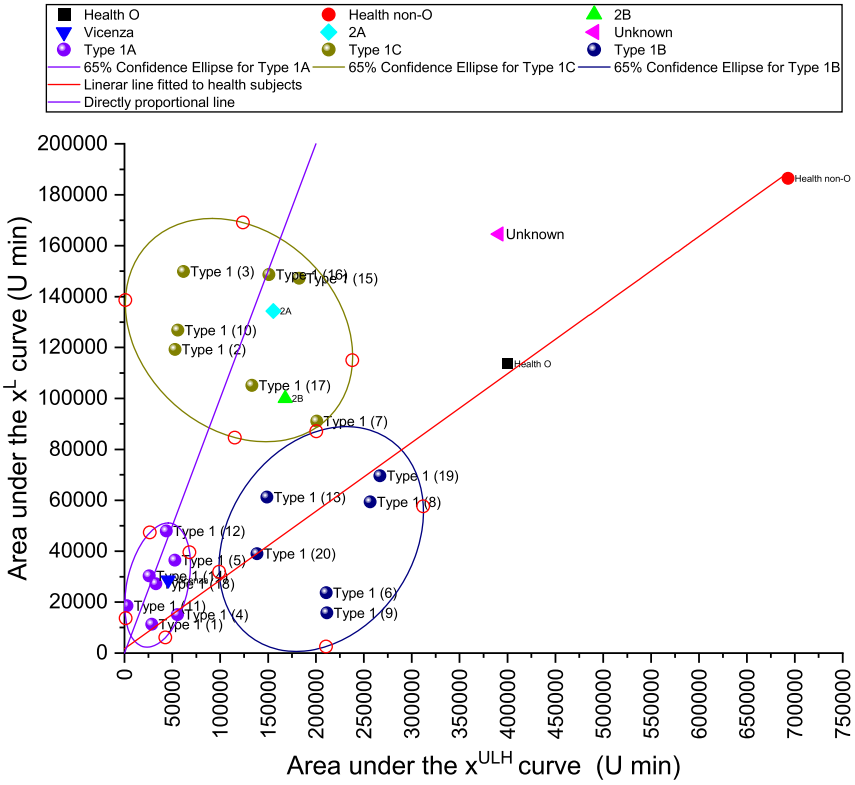

Figure 11.7: Analysis of the area under the curve (AUC) for LMW and (UL + HMW) multimers as computed by the Ferrari et al. [14] model. Lines show proportionality relationships between AUCs in selected classes.

2. Type 1B (blue balls): characterised by higher VWF levels and quasi-normal multimeric distribution, normal proteolytic activity but high clearance (associated with mutations R1205H, C1130G/F/R, W1144G);
3. Type 1C (green balls): characterised by high VWF levels but limited amount of HMW multimers, increased release (mutations G160W, N166I, L2207P), increased clearance (mutations R1205H, C1130G/F/R, W1144G) and accelerated proteolysis (mutation C1584).

The understanding of the relationship between PK parameters and mutations in type 1 VWD [32, 33] represents an open area of research, because mechanistic models have the potential to clarify and quantify the prevalent metabolic pathways involved in each type 1 subtype.

11.6 Model-based design of clinical tests

Information content analysis can be executed on both the post-DDAVP models of VWD (see Section 11.4.2) and on PK models of VWD including exogenous infusion (Section 11.4.3) with the following goals: *i*) study the distribution of information during clinical tests and evaluate the impact of information distribution on the overall test duration required to precisely estimate the set of PK parameters; *ii*) suggest the optimal infusion policy and/or allocation of sampling times for VWF:Ag and VWF:CB measurements; *iii*) quantify and rank the relative information that can be obtained using different VWF concentrates. The metric that is used to evaluate the overall information content of a clinical test is the trace of dynamic Fisher Information Matrix (FIM), which is defined by

$$I_d\left(\hat{\boldsymbol{\theta}}, t\right) = tr\left[\mathbf{H}_\theta\left(\hat{\boldsymbol{\theta}}, t\right)\right] \tag{11.22}$$

In Equation (11.22), $\mathbf{H}_\theta$ is the dynamic FIM calculated at the estimated value of model parameters, which are calculated from

$$\mathbf{H}_\theta\left(\hat{\boldsymbol{\theta}}, t\right) = \left[\mathbf{V}_\theta\left(\hat{\boldsymbol{\theta}}, t\right)\right]^{-1} \cong \sum_{j=1}^{N_m}\left[\frac{1}{\sigma_j^2}\left(\frac{\partial \hat{y}_j\left(\hat{\boldsymbol{\theta}}, t\right)}{\partial \theta_k}\,\frac{\partial \hat{y}_j\left(\hat{\boldsymbol{\theta}}, t\right)}{\partial \theta_l}\right)\right]_{k,l=1\ldots N_\theta} \tag{11.23}$$

In Equation (11.23), the FIM, which is the inverse of the variance-covariance matrix of model parameters $\mathbf{V}_\theta$, is expressed as the product of the sensitivity of the *j*-th output variable with respect to each of the N_θ parameter in the conditions investigated in the *i*-th test, divided by the corresponding variance of measurement error (σ_j^2) for the *j*-th measured response (VWF:Ag or VWF:CB). Sensitivity coefficients appearing in (11.23) are calculated by integrating the sensitivity equations alongside the model equations as described in Bard [30]. Information from (11.23) can be decomposed to analyse the contribution to the information related to the estimation of the *i*-th model parameter (h_{ii}):

$$I_d\left(\hat{\boldsymbol{\theta}}, t\right) = tr\left[\mathbf{H}_\theta\left(\hat{\boldsymbol{\theta}}, t\right)\right] = \sum_{i=1}^{N_\theta} h_{ii}\left(\hat{\boldsymbol{\theta}}, t\right) \tag{11.24}$$

A maximum in I_d defines the most informative time points to take samples during the clinical test. When this maximum is located at the end of the test, information acquisition is favoured by long test durations. If an information peak is located at the very beginning of the test, samples can be concentrated in the first few hours of test execution and the test duration can significantly be reduced. Optimal sampling allocation can be obtained by solving the following optimal model-based design of experiments (MBDoE) problem [34]:

$$\mathbf{t}^{sp} = \text{argmin}\psi[\mathbf{V}_\theta] = \text{argmin}\psi\left[\left(\sum_{i=1}^{N_{sp}} \mathbf{H}_\theta(\theta, t_i)\right)^{-1}\right] \tag{11.25}$$

where $\mathbf{t}^{sp} = \begin{bmatrix} t_1 & t_2 & \dots & t_{N_{sp}} \end{bmatrix}$ is the optimal vector of sampling times and ψ [.] is a metric function of the variance-covariance matrix of model parameters, identifying the chosen experimental design criterion. Popular choices for ψ are the determinant (D-optimality), the trace (A-optimality), the largest eigenvalue (E-optimality) of $\mathbf{V}_\theta$ [35]. The optimisation in (11.25) is carried out considering practical constraints on sampling points allocation in time, including, for fixed number of samples N_{sp}: *i*) minimum time between consecutive measurements; *ii*) test duration. This set of constraints $\mathbf{C} = [C_{1\text{i}}\ C_2]$ are formulated as

$$C_{1i} = \Delta t_i = t_i - t_{i-1} \geq MTBM\ i = 1 \dots N_{sp} \tag{11.26}$$

$$C_2 = \sum_{i=1}^{N_{sp}} \Delta t_i \leq \tau^{MAX} \tag{11.27}$$

where MTBM is the minimum time between consecutive measurements (here set to 15 min to propose a practical, clinically feasible test) and τ^{MAX} is the maximum allowed duration for the test (here fixed to 24 h, which is the maximum duration of a standard DDAVP test). If multiple infusion is considered, the optimal experimental design problem can be written as

$$\{\mathbf{t}^{sp}, \mathbf{D}^{IV}, \mathbf{t}_{inj}\} = \text{argmin}\psi[\mathbf{V}_\theta] = \text{argmin}\psi\left[\left(\sum_{i=1}^{N_{sp}} \mathbf{H}_\theta(\theta, t_i)\right)^{-1}\right] \tag{11.28}$$

and the objective is to determine the optimal experimental decision variables (elements of the experimental design vector) including optimal sampling times ($\mathbf{t}^{sp}$), injection times ($\mathbf{t}_{inj}$) and infusion rates ($\mathbf{D}^{IV}$). The optimisation (25) or (28) subject to (20) and (21) and the model equations (11.8)–(11.10) including (4–6) and (11) is carried out using the gPROMS ModelBuilder software [31] using a sequential quadratic programming (SQP) optimisation solver with multiple shooting to solve the resulting NLP problem.

11.7 Design of single and multiple infusion tests for the treatment of AVWS

11.7.1 Preliminary parameter estimation from DDAVP and VWF infusion tests data

Data available for a subject affected by AVWS have been used to calibrate the DDAVP model by Ferrari and coworkers [14] and the Galvanin et al. [21] models including VWF

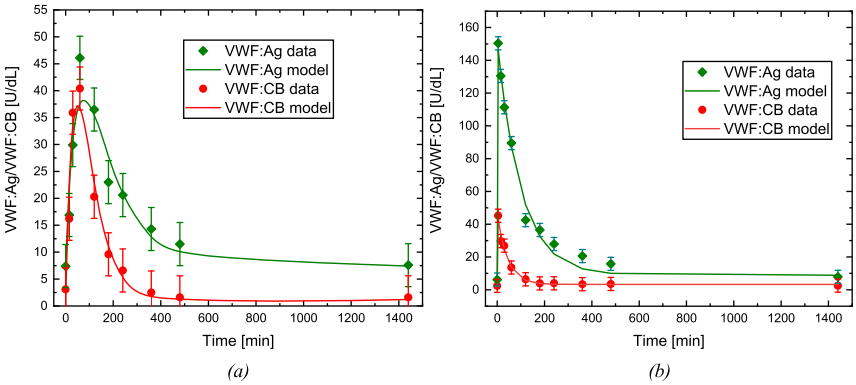

Figure 11.8: Model identification results from AVWS data using (a) the post-DDAVP model proposed by Ferrari et al. [14] and (b) the model proposed by Galvanin et al. [21] including exogenous VWF infusion. VWF:Ag and VWF:CB measurements are indicated, respectively, by green diamonds and red circles; error bars indicate the standard deviation in the data.

infusion. Results after model identification are illustrated in Figure 11.8a (post-DDAVP test) and Figure 11.8b (Haemate P administration test).

Parameter estimation results are reported in Table 11.4. Results show that both models are adequately fitting the available clinical data, providing very limited deviations from the measured VWF:Ag and VWF:CB concentrations, as underlined by the corresponding low χ^2 values reported in Table 11.4. A more detailed analysis of residuals reveal that the post-DDAVP model has some minor limitations on representing the initial VWF:Ag peak observed in the clinical test, while the infusion model tends to underestimate the observed VWF:Ag decay realised after 5–8 h from VWF infusion. Results from

Table 11.4: Estimated values of model parameters and a-posteriori statistics, including 95 % confidence intervals, *t*-test and χ^2 lack of fit test results for the post-DDAVP model and Haemate P infusion model. Asterisk* and bold values indicate parameters failing the *t*-test [21].

Post-DDAVP model				Haemate P infusion model			
Model parameters	**Estimated value**	**Confidence interval**	***t*-value (Ref: 1.75)**	**Model parameters**	**Estimated value**	**95 % Confidence interval**	***t*-value (Ref: 1.73)**
k_1	0.01092	0.0044	2.13	k_1	0.01248	0.0049	2.53
k_e	0.00845	0.0042	2.49	k_e	0.00990	0.0005	18.60
k_0	0.02051	0.0095	1.98	D_{IV}	1658.254	8913.9784	**0.186***
D	1304.1110	762.5731	**1.71***	t_{inj}	2.7228	14.4830	**0.188***
t_{max}	219.6	10980.0105	**0.02***	–	–	–	–
χ^2	23.3	χ^2_{ref}	26.3	χ^2	25.5	χ^2_{ref}	28.9

parameter estimation (Table 11.4) show that the available clinical data allow a precise estimation of the key haemostatic parameters for the description of proteolysis (parameter k_1) and elimination (parameter k_e) pathways, as confirmed by the low 95 % confidence intervals. However, the description of release parameters D and $t_{\max}$ (post-DDAVP model) and infusion parameters D_{IV} and t_{inj} (Haemate P infusion model) is more difficult, due to the strong correlation and the limited amount of data points available to capture the initial transient behaviour observed after drug administration. Interestingly, the Haemate P infusion test allows for a more precise estimation of the elimination parameter k_e compared to a standard DDAVP test, while there are no significant differences when comparing the precision in the estimate for proteolytic parameter k_1.

By analysing the estimates for key parameters k_1 and k_e (Figure 11.9), it is apparent that the estimated parameter values obtained from the two different tests (DDAVP and Haemate P infusion) are very similar, and undistinguishable considering the uncertainty in parameter estimates. As illustrated in the figure, the AVWS subject shows accelerated proteolysis and elimination pathways compared to healthy control subjects, resulting in a lack of high molecular weight species in the blood stream and, consequently, a reduced haemostatic activity. A precise estimation of k_e and k_1 (minimum variance in the estimation of these parameters) is crucial for the model-based diagnosis of the subject and to achieve a clear distinction between AVWS subjects and subjects affected by other types of VWD.

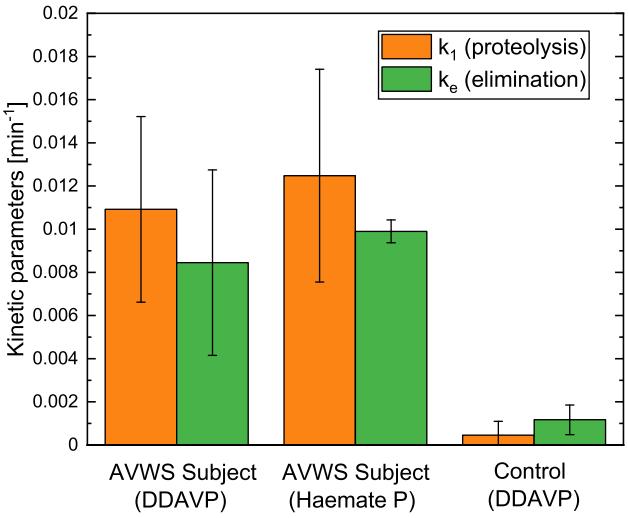

Figure 11.9: Parameter estimation results for key haemostatic parameters related to proteolysis (k1) and elimination (k_e) of VWF from plasma for the AVWS subject after DDAVP and Haemate P infusion, and comparison with healthy (O + non-O) control subjects. Bars on columns indicate 95 % confidence intervals [21].

11.7.2 Optimal design of Haemate P administration tests including single and multiple infusion

Results from parameter estimation illustrated in Section 11.7.1 showed a limitation of current infusion protocols to estimate the full set of model parameters (k_e, k_1 and D_{IV}) precisely. To overcome this limitation, a D-optimal MBDoE has been carried out to design alternative infusion protocols:

- **Protocol 1**: design of single infusion test where the objective is to optimise the allocation of sampling points, while the infusion rate is estimated to deliver a dose of q = 4500 U;
- **Protocol 2**: design of a multiple infusion test where the objective is to determine the optimal allocation of sampling points ($\mathbf{t}^{sp}$) in time, time for three injections ($\mathbf{t}_{inj}$) and corresponding infusion rates for the injections ($\mathbf{D}^{IV}$).

For Protocol 1 and Protocol 2, the corresponding optimal experimental design optimisation problems are defined by equations (11.25) and (11.28), respectively, subject to (20) and (21) and the model equations (11.8)–(11.10) including (11.4–11.6) and (11.11). In the everyday clinical procedures, there is a non-negligible uncertainty in the definition of each sample measurement, as it is impractical to sample with a resolution in time lower than 10 min. Therefore, a conservative constraint on the minimum time between measurements of 15 min has been assumed in the MBDoE optimisation. Optimal experimental design results are illustrated in Table 11.5 in terms of experimental design variables and test duration. Figure 11.10 shows the simulated VWF:Ag and VWF:CB profiles and the optimal allocation of samples determined by MBDoE for Protocol 1. As expected, given the faster information dynamics realised in infusion experiments, the sampling points are

Table 11.5: Allocation of sampling points in time and duration for DDAVP, Haemate P infusion and D-optimal designed Haemate P infusion tests.

Test protocol	Administration	Experimental design variables	Test duration [h]
DDAVP	**Standard dose DDAVP**	$\mathbf{t}^{sp}$ = [0 15 30 60 120 180 240 360 480 1440] [min]	24
Haemate P infusion	**Standard Haemate P dose single infusion**	$\mathbf{t}^{sp}$ = [0 4 15 30 60 120 180 240 360 480 1440] [min]	24
D-optimal MBDoE Haemate P infusion	**Optimised Haemate P dose single infusion**	$\mathbf{t}^{sp}$ = [0 15 30 45 60 75 90 105 120 135 150] [min]	2.50
D-optimal MBDoE Haemate P infusion	**Optimised Haemate P doses multiple infusion**	$\mathbf{t}^{sp}$ = [0 17 33 48 63 78 93 108 123 138 153] [min] $\mathbf{t}_{inj}$ = [0 42 83] [min] $\mathbf{D}^{IV}$ = [1407 1418 1416] [U/min]	2.54

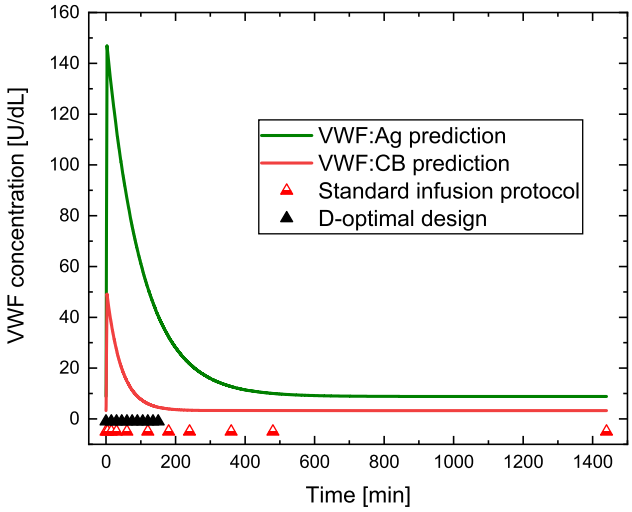

Figure 11.10: Protocol 1: predicted profiles of VWF:Ag and VWF:CB and allocation of sampling points as obtained from the D-optimal designed test (black triangles) as compared to the original allocation of sampling points in standard Haemate P infusion tests (red circles) [21].

concentrated at the very beginning of the test. Albeit not shown for the sake of conciseness, this result does not change significantly if different experimental design criteria are used (i.e. A- or E-optimal).

Results in terms of parameter estimation for Protocol 1 are reported in Table 11.6. It is interesting to verify that, if we assume that a precise injection time can be guaranteed during the infusion, i.e. by fixing the infusion time at t_{inj} = 3 min, a precise estimation of all key parameters k_1, k_e and D_{IV} can be achieved. Results show that Protocol 1 is more efficient to precisely estimate the kinetic parameters k_1 and k_e when compared to the original sampling used in Haemate P infusion tests (see Table 11.4), as demonstrated by the reduced confidence intervals in D_{IV}, while preserving a similar value in the other estimated parameters. Most importantly, note that this optimal sampling schedule (as the

Table 11.6: Protocol 1: estimated values of model parameters and a-posteriori statistics, including 95 % confidence intervals, *t*-test and χ^2 lack of fit test results obtained from the D-optimally designed Haemate P infusion test assuming a fixed injection time (t_{inj} = 3 min) [21].

Haemate P infusion model after MBDoE (Protocol 1)			
Model Parameters	**Estimated value**	**95 % Confidence Interval**	**t-value (Ref: 1.73)**
k_1	0.0140	0.0078	1.80
k_e	0.0099	0.0020	4.99
D_{IV}	1658.2500	159.9083	10.37
χ^2	23.7	χ^2_{ref}	28.9

one realised in Protocol 2) would require a considerably shorter test than the currently adopted infusion protocol (150 min–2.5 h against 24 h of the currently proposed infusion test), maintaining the same level of information for the determination of key PK parameters. Results show that a small variation in the injection time from 2.7 s (as reported in Table 11.4) to 3 s does not affect the estimated values of model parameters, but it slightly affects the precision of the estimates for parameters k_1 and k_e while the LOF test is passed and does not change significantly if t_{inj} is affected by uncertainty, as the test kinetics are very fast during the intravenous drug administration of Haemate P.

Results for Protocol 2 are reported in terms of infusion rate (Figure 11.11a) and VWF concentration profiles (Figure 11.11b). If a multiple administration of Haemate P is optimally designed using MBDoE, the injection times are concentrated in the first 1.2 h of the test and the design suggests a similar infusion rate for the three Haemate P injections.

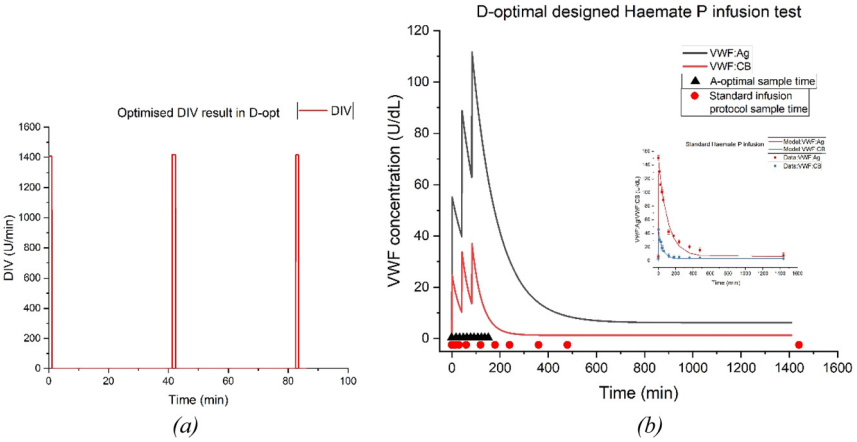

Figure 11.11: Protocol 2: (a) profile of Haemate P infusion rate as obtained from a D-optimal MBDoE optimisation; (b) predicted profiles of VWF:Ag and VWF:CB and allocation of sampling points as obtained from the D-optimal designed test (black triangles) as compared to the original allocation of sampling points in standard Haemate P infusion tests (red circles and inset figure).

Table 11.7: Protocol 2: estimated values of model parameters and a-posteriori statistics, including 95 % confidence intervals, *t*-test and χ^2 lack of fit test results obtained from the D-optimally designed Haemate P infusion test including multiple infusion assuming a fixed injection time (t_{inj} = 3 min).

Haemate P infusion model after MBDoE (Protocol 2)			
Model parameters	**Estimated value**	**95 % Confidence interval**	***t*-value (Ref: 1.73)**
k_1	0.0145	0.0022	6.38
k_e	0.0094	0.0003	36.3
χ^2	21.7	χ^2_{ref}	28.9

Results from parameter estimation (Table 11.7) show a significant improvement in terms of precision of the estimates (compare Table 11.7 with Table 11.6) in the identification of k_1 and k_e parameters. However, this protocol requires an accurate administration of the VWF analogue and represents a more invasive procedure for the subject. These factors should be taken into account when implementing this optimally designed test in clinical facilities.

11.8 Conclusions

VWD is a very heterogeneous disease whose diagnosis requires a significant number of tests and experience, particularly when subjects are affected by specific VWD forms. The availability of PK models that can be tailored to the specificity of the single subject affected by VWD represents a key opportunity to achieve a quantitative description of the VWF multimer distribution for a faster and more effective diagnosis from clinical data. Model-based diagnosis has shown very promising results on identifying subjects affected by main VWD types, with type 1 VWD still offering a major challenge in the classification of VWD subtypes, given the strong heterogeneity of this specific VWD type. However, kinetic models can be affected by several limitations: *i*) often their calibration requires a 24 h-long tests (DDAVP test for example) to achieve a statistically satisfactory estimation of the PK metabolic parameters for each subject; *ii*) so far most of the PK models have been developed based on a fixed drug administration dose, while models including exogenous infusion of VWF concentrates, which represent the main form of treatment for severe forms of VWD, have found (so far) limited clinical application. New VWD models including exogenous VWF infusion have been recently proposed to bridge this research gap [21] and to provide a precise identification of haemostatic parameters from treatment tests. It has been shown that MBDoE techniques can be used to redesign currently adopted Haemate P infusion tests by optimally allocating the sampling points to maximise the information acquired during an infusion test. Results show that using MBDoE new clinically feasible sampling protocols can be designed where the test duration can successfully be reduced from 24 h to 2.5 h and where the injection time can be controlled to precisely estimate the full set of individual PK parameters. The possibility to reduce test duration associated to a conventional infusion test is a remarkable achievement. It allows patients to undergo a less stressful clinical procedure and facilitates clinical management in terms of both economical and organisational aspects. The precise estimation of individual haemostatic parameters allows to obtain a subject-specific calibrated model that can be used for personalised disease monitoring to improve the dosage of VWF concentrates, a key aspect to address when treating severe forms of VWD. Future work will aim to *i*) extend the applicability of the infusion models to other VWD types by implementing new MBDoE-optimised protocols in clinical facilities and estimating key PK parameters for new subjects affected by VWD; *ii*) design clinical tests that are more flexible and less stressful for the subjects; *iii*) consider the effect of

model mismatch in the optimal experimental design formulation [36] so that the feasibility of the MBDoE-designed test [37] can be guaranteed even in scenarios of clinical uncertainty.

Acknowledgements: The authors would like to thank the editors David Bogle and Tomasz Sosnowski for their guidance and review of this article before its publication.

References

1. Lillicrap D, Budde U, Jessat U, Zimmerman R, Simon M, Kätzel R, et al. Von Willebrand disease-phenotype versus genotype: deficiency versus disease. Thromb Res 2007;87:57–64.
2. Sadler JE. Von Willebrand disease type 1: a diagnosis in search of a disease. Blood 2003;101:2089–93.
3. Sadler JE, Mannucci PM, Berntorp E, Bochkov N, Boulyjenkov V, Ginsburg D, et al. Impact, diagnosis and treatment of von Willebrand disease (2000). Thromb Haemost;84:160–74. https://doi.org/10.1055/s-0037-1613992.
4. World Federation of Haemophilia (WFH). Report on the annual global survey. WFH Reports 2020.
5. Rodeghiero F, Castaman G, Dini E. Epidemiological investigation of the prevalence of von Willebrand's disease. Blood 1987;69:454–9.
6. National Institute of Health. The Diagnosis, Evaluation and Management of von Willebrand Disease. National Institute of Health Reports 2008.
7. Groot E, Fijnheer R, Sebastian S, De Groot P, Lenting P. The active conformation of von Willebrand factor in patients with thrombotic thrombocytopenic purpura in remission. J Thromb Haemostasis 2009;7:962–9.
8. Atiq F, Heijdra J, Snijders F, Boender J, Kempers E, van Heerde WL, et al. Desmopressin response depends on the presence and type of genetic variants in patients with type 1 and type 2 von Willebrand disease. Blood Adv 2022;6:5317–26.
9. Tiede A, Rand JH, Budde U, Ganser A, Federici AB. How I treat the acquired von Willebrand syndrome. Blood 2011;117:6777–85.
10. Galletta E, Galvanin F, Bertomoro A, Daidone V, Casonato A. Acquired von Willebrand syndrome in patients with monoclonal gammopathy of undetermined significance investigated using a mechanistic approach. Blood Transfus 2021. https://doi.org/10.2450/2021.0121-21.
11. Casonato A, Daidone V, Padrini R. Assessment of von Willebrand factor propeptide improves the diagnosis of von Willebrand disease. Semin Thromb Hemost 2011;37:456–63.
12. Gezsi A, Budde U, Deak I, Nagy E, Mohl A, Schlammadinger A, et al. Accelerated clearance alone explains ultra-large multimers on von Willebrand disease Vicenza. J Thromb Haemostasis 2010;8:1273–80.
13. Galvanin F, Barolo M, Padrini R, Casonato A, Bezzo F. A model-based approach to the automatic diagnosis of von Willebrand disease. AIChE J 2014;60:1718–27.
14. Ferrari M, Galvanin F, Barolo M, Daidone V, Padrini R, Bezzo F, et al. A Mechanistic Model to Quantify von Willebrand Factor Release, Survival and Proteolysis in Patients with von Willebrand Disease. Thromb Haemost 2018;118:309–19.
15. Taverna B, Casonato A, Bezzo F, Galvanin F. A framework for the optimal design of a minimum set of clinical trials to characterize von Willebrand disease. Comput Methods Progr Biomed 2019;179:104989.
16. Castaldello C, Galvanin F, Casonato A, Padrini R, Barolo M, Bezzo F. A model-based protocol for the diagnosis of von Willebrand disease. Can J Chem Eng 2018;96:628–38.
17. Casonato A, Pontara E, Sartorello F, Cattini MG, Gallinaro L, Bertomoro A, et al. Identifying type Vicenza von Willebrand disease. J Lab Clin Med 2006;147:96–102.

18. Budde U, Metzner HJ, Muller HG. Comparative analysis and classification of von Willebrand factor/factor VIII concentrates: impact on treatment of patients with von Willebrand disease. Semin Thromb Hemost 2006;32:626–35.
19. Berntorp E. Haemate P/Humate-P: a systematic review. Thromb Res 2009;124:S11–4.
20. Auerswald G, Kreuz W. Haemate P/Humate-P for the treatment of von Willebrand disease: considerations for use and clinical experience. Haemophilia 2008;14:39–46.
21. Galvanin F, Galletta E, Bertomoro A, Daidone V, Casonato A. Optimal design of infusion tests for the identification of physiological models of acquired von Willebrand syndrome. Chem Eng Sci 2024:119660. https://doi.org/10.1016/j.ces.2023.119660.
22. Villaverde AJ, Pathirana D, Fröhlich F, Hasenauer J, Banga JR. A protocol for dynamic model calibration. Briefings Bioinf 2022;23:1–19.
23. Franceschini G, Macchietto S. Novel anticorrelation criteria for model-based experiment design: theory and formulations. AIChE J 2008;54:1009–24.
24. Chakrabarty A, Buzzard GT, Rundell AE. Model-based design of experiments for cellular processes. Syst Biol Med 2013;5:181–203.
25. Favaloro EJ, Thom J, Patterson D, Just S, Dixon T, Koutts J, et al. Desmopressin therapy to assist the functional identification and characterisation of von Willebrand disease: differential utility from combining two (VWF: CB and VWF:RCo) von Willebrand factor activity assays? Thromb Res 2009;123:862–8.
26. Casonato A, Gallinaro L, Cattini MG, Sartorello F, Pontara E, Padrini R, et al. Type von Willebrand disease due to reduced von Willebrand factor synthesis and/or survival: observations from a case study. Transl Res 2010;155:200–8.
27. Menache D, Aronson DL, Darr F, Montgomery RR, Gill JC, Kessler CM, et al. Pharmacokinetics of von Willebrand factor and factor VIIIC in patients with severe von Willebrand disease (type 3 VWD): estimation of the rate of factor VIIIC synthesis. Br J Haematol 1996;94:740–5.
28. Casonato A, Pontara E, Sartorello F, Cattini MG, Sartori MT, Padrini R, et al. Reduced von Willebrand factor survival in type Vicenza von Willebrand disease. Blood 2002;99:180–4.
29. Snedecor GW, Cochran WG. Statistical methods, 8th ed. Ames: Iowa State University Press; 1989.
30. Bard Y. Nonlinear parameter estimation. Cambridge, USA: Academic Press; 1974.
31. Siemens Process Systems Enterprise. gPROMS 2023. https://www.siemens.com/global/en/products/automation/industry-software/gproms-digital-process-design-and-operations.html.
32. Goodeve AC. The genetic basis of von Willebrand disease. Blood Rev 2010;24:123–34.
33. Goodeve A. Genetics of type 1 von Willebrand disease. Curr Opin Hematol 2007;14:444–9.
34. Fedorov V, Leonov S. Optimal design for nonlinear response models. Boca Raton: Taylor & Francis Group; 2014.
35. Pukelsheim F. Optimal design of experiments. Boca Raton, USA: Chapman & Hall; 1995.
36. Galvanin F, Barolo M, Macchietto S, Bezzo F. Optimal design of clinical tests for the identification of physiological models of type 1 diabetes in the presence of model mismatch. Med Biol Eng Comput 2011;49:263–77.
37. Galvanin F, Bezzo F. Advanced techniques for the optimal design of experiments in pharmacokinetics. Comput Aided Chem Eng 2018;42:65–83.